[1]Yueqiang Wang

Landscape Design and Green Space Perception Enhancement Based on Panoramic Imaging and Segnet

Journal of Electrical Systems

Abstract: - Green view rate is an intuitive evaluation criterion used for green space perception. Traditional research on green view rate is mostly calculated based on flat images, which cannot fully reflect the subjective human perception of green volume in three-dimensional space. Based on the panoramic image, we propose the concept of panoramic green perception rate, obtain spherical panoramic photos by panoramic camera, convert isometric cylindrical projection into isoprojective cylindrical projection, and use the convolutional neural network model based on semantic segmentation to automatically identify the area of vegetation to achieve automatic recognition and measurement of panoramic green perception rate. The results were compared with manual discrimination and showed that the average intersection ratio (mIoU) of greenery recognition using Dilated ResNet-105 was 62.53%, and the average difference with manual recognition was 9.17%.

Keywords: Landscape gardening, Green-visibility, Deep learning, Semantic segmentation.

I. INTRODUCTION

In contemporary urban planning and design, there is a growing recognition of the importance of integrating rural areas into the broader framework of human settlement development. Rural landscapes, often characterized by their unique natural features and cultural heritage, play a crucial role in shaping the overall environmental quality and sustainability of human settlements. However, effectively planning and designing rural landscapes require a comprehensive understanding of the complex interplay between spatial and temporal dynamics, as well as the diverse socio-economic factors influencing rural communities[1,2].

In recent years, advancements in spatial data analysis techniques have provided valuable tools for studying and understanding rural landscapes in greater detail. By leveraging geospatial technologies and analyzing spatiotemporal data, planners and designers can gain insights into the evolving patterns of land use, environmental changes, and community dynamics within rural areas. This enables a more holistic approach to landscape planning and design that takes into account the unique characteristics and needs of rural communities[3,4].

This paper aims to explore the application of rural spatiotemporal data analysis in human settlement environment landscape planning and design. Drawing upon interdisciplinary research in geography, environmental science, and urban planning, we seek to elucidate the potential benefits of integrating advanced data analytics techniques into the planning and design process. Through case studies and practical examples, we will demonstrate how spatial data analysis can inform decision-making, enhance stakeholder engagement, and promote sustainable development practices in rural areas[5,6,7].

Deep learning (DL) refers to learning the intrinsic laws and levels of representation of sample data so that machines can have the same analytical learning ability as humans and can recognise data such as text, images and sound[8-10]. At present, deep learning has gained wider application in the field of artificial intelligence technology [11-15]. With the development of deep learning techniques in recent years, a series of open source convolutional neural network (CNN) models for semantic segmentation of images have emerged. This study analyses and compares existing CNN models commonly used in landscape gardening to identify vegetation parts in panoramic images to automate the calculation of green view rate[16-18].

By highlighting the significance of rural spatiotemporal data analysis in landscape planning and design, this research contributes to ongoing efforts to create more resilient, inclusive, and environmentally sustainable human settlements. Through collaboration between researchers, practitioners, and local communities, we can harness the

[1] School of Architecture and Environmental Arts, Shanghai Urban Construction Vocational College, Shanghai 201415, China;

*Corresponding author:wangyueqiang2024@163.com;

power of data-driven insights to shape landscapes that not only meet the needs of current generations but also preserve the natural and cultural heritage for future generations to enjoy.

II. MEASUREMENT AND CALCULATION OF PANORAMIC GREEN-VISIBILITY

Based on the panoramic image, this study proposes a methodological step to calculate the panoramic green view rate, including panoramic image acquisition, panoramic image projection transformation, visible vegetation area calculation.

A. Panoramic image acquisition

Panoramic images can be acquired in 2 ways: by conventional cameras and by multi-lens panoramic cameras.

A conventional camera is used to photograph each sample point and take pictures at the same angle every other time along the horizontal direction, so that the preliminary images are combined with multiple visual angles of the sample point. In other words, the photos are combined according to the visual characteristics[19]. However, this method is complicated and requires post-processing.

Using panoramic filming equipment, such as multi-lens panoramic cameras, to obtain panoramic images directly. With the development of VR and the video industry, panoramic equipment is becoming more and more widely used and direct filming with panoramic cameras will be a future trend[20].

B. Panoramic image projection transformation

The panoramic image obtained by a panoramic camera or associated equipment is generally an equirectangular projection. The projection spread is a 2:1 rectangular image. In an equirectangular projection, areas with equal projected areas do not have equal true areas[21]. In order to make the area of the panoramic image measurable, it is necessary to convert it into a cylindrical equal-area projection for calculation. This is done by first converting the original equidistant cylindrical projection to spherical coordinates and then converting the spherical coordinates to the equivalent cylindrical projection[22].

An equidistant cylindrical projection is a projection in which the cylindrical projection plane is parallel to the earth's axis, and a network of warp and weft lines is projected onto the cylindrical plane under the condition that the length of the warp lines remains constant, and then dissected and flattened along one of the bus bars. These projections have latitudinal and longitudinal intervals equal to the field, and the meridians and latitudes are shown as equidistant parallel lines perpendicular to each other [23] (Fig. 1).

Fig. 1 Isometric cylindrical projection

Equation for converting isometric cylindrical projections to spherical latitude and longitude coordinates:

$$\lambda = x_1 / \left(\cos \phi_1\right) + \lambda_0 \quad (1)$$

$$\phi = y_1 + \phi_1 \quad (2)$$

Where λ is the longitude of the location of the fixed point in spherical coordinates, ϕ is the latitude of the location of the fixed point in spherical coordinates, ϕ_1 is the standard latitude line in spherical coordinates, λ_0 is the central longitude line in spherical coordinates, x_1 is the horizontal coordinate of the equidistant cylindrical projection position, and y_1 is the vertical coordinate of the equidistant cylindrical projection position.

The isometric cylindrical projection is transformed to produce a panoramic sphere (Fig. 2).

Fig. 2 Panoramic sphere

The equiprojected cylindrical projection is a projection on a cylinder tangent to the equator of the panoramic sphere under the condition of equal area, where the meridians are equidistant parallel lines and the latitude lines are parallel lines perpendicular to the meridians and at intervals that decrease in spacing with increasing latitude (Fig. 3).

Fig. 3 Equiprojected cylindrical projection

Equation for converting a panoramic sphere to an equiprobable cylindrical projection:

$$x_2 = (\lambda - \lambda_0)\cos\lambda_0 \quad (3)$$

$$y_2 = \sin\phi / \cos\lambda_0 \quad (4)$$

Where λ is the longitude of the location of the panoramic sphere, ϕ is the latitude of the location of the panoramic sphere, λ_0 is the central meridian of the panoramic sphere, x_2 is the horizontal coordinate of the equiprojected cylindrical position, and y_2 is the vertical coordinate of the equiprojected cylindrical position.

III. AUTOMATIC RECOGNITION OF PANORAMIC GREEN VIEWS

A. Semantic segmentation neural network features

Neural network models are mathematical models that analyse, learn and parse data by simulating the way human brain neurons process information. CNN are a type of feedforward neural network and are widely used in image recognition, usually consisting of a fully connected layer at the top, one or more convolutional layers and a pooling layer [6].

Neural networks for image processing need to go through five major steps: image pre-processing, image compression, image feature extraction, image segmentation and image recognition [7], and have the following characteristics: fast processing speed; strong adaptive ability; can build mathematical models to analyse image information; can handle non-linear problems in images; can pre-process noise or impurity data in images, etc [8].

Semantic segmentation is a common operation in image analysis, describing the process of associating each pixel of an image with a type of label (e.g. flower, person, road, etc.) (Figure 4), which is commonly used in areas such as autonomous driving, industrial monitoring, remote sensing image classification, and medical image analysis.

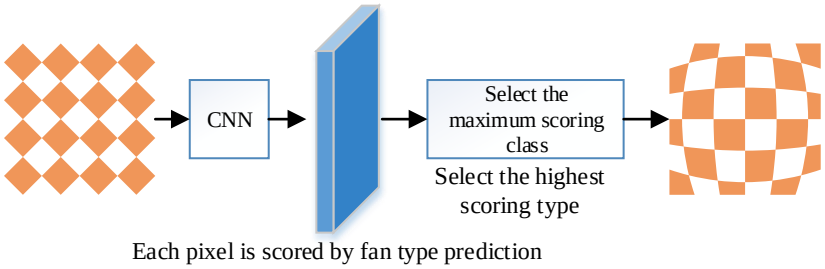

Fig. 4 Neural network model image semantic segmentation process

B. Semantic segmentation models for images

SegNet's semantic segmentation architecture preserves the index of the pooling layer when the encoder portion of the image is downscaled, allowing the integrity of high frequency details to be maintained in the segmentation [9]. Compared to other semantic segmentation networks, this architecture is trained by convolutional operations and is a lightweight network with fewer parameters. In this paper, we train a semantic segmentation model of riverfront images based on the SegNet network structure for the riverfront greenway landscape garden, and classify the riverfront greenway landscape garden labels into 13 categories, namely grass, trees, water bodies, sky, barge, landscape garden structures, roads, vehicles, buildings, guardrails, bridges, people, and others (litter bins, warning signs, miscellaneous objects, etc.).

The flow of the image semantic segmentation (Figure 5) is as follows:

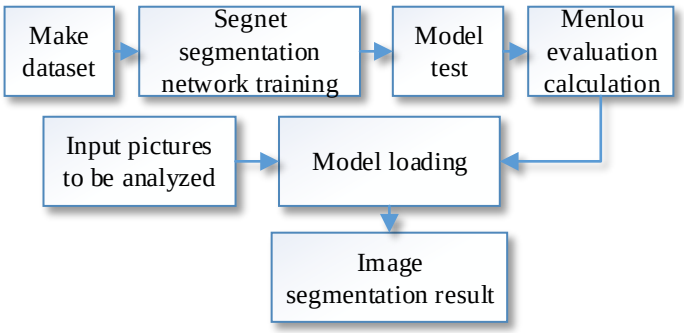

Fig. 5 Construction process of semantic segmentation model of waterfront landscape image

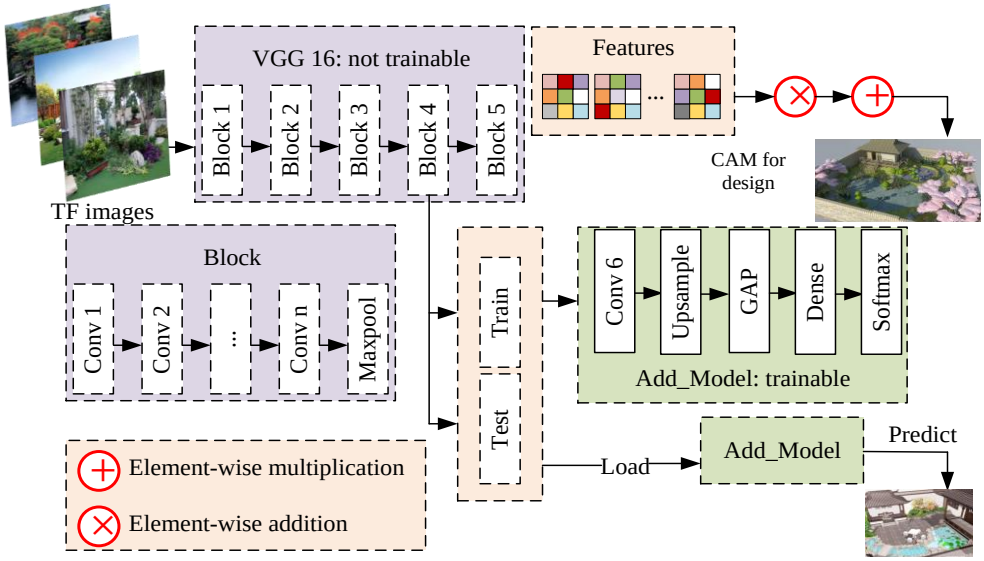

Fig. 6 Model for this paper

The model in this paper is shown in Figure 6, where the pixel points are classified and labelled. A dataset was generated by selecting 90 panoramic images of the riverfront and labelling them in matlab with 13 types of landscape garden element labels. The dataset was trained with SegNet segmentation network. After 100 generations of training, the accuracy of the model was verified according to Eqs. (5) to (8), and the model was loaded to generate image segmentation results on the basis of the accuracy achieved.

$$A_i = \frac{P_{ii}}{P_{ij}} \quad (5)$$

$$\mathrm{IoU}_i = \frac{P_{ii}}{P_{ij} + P_{ji} - P_{ii}} \quad (6)$$

$$\mathrm{PA} = \frac{\sum_{i=0}^{k} P_{ii}}{\sum_{i=0}^{k}\sum_{j=0}^{k} P_{ij}} \quad (7)$$

$$\mathrm{MIoU} = \frac{1}{k+1}\sum_{i=0}^{k} \frac{P_{ii}}{\sum_{j=0}^{k} P_{ij} + \sum_{j=0}^{k} P_{ji} - P_{ii}} \quad (8)$$

Where k is the total number of landscape garden tag categories, A_i is the accuracy of true pixel category i, IoU_i is the total number of pixels of true pixel category i predicted P_{ii} to category i, P_{ji} is the total number of pixels of true pixel category i predicted to category j, P_{ji} is the total number of pixels of true pixel category j predicted to category i, PA is the overall pixel accuracy, and MIoU is the average intersection ratio.

C. Visual perception analysis

In planning guidance studies, multiple linear regression models are used to determine the closeness of relationships between multiple variables and hence the correlation [3]. Based on the results of selected landscape garden features and visual perception measures of the waterfront greenway, a multiple linear regression analysis model (Equation (9)) was constructed using the statsmodel software package in python to test the correlations between the ten

evaluation criteria and the visual perception scores to investigate the extent to which each criterion influenced the visual perception results and the correlations between different landscape garden features and visual perception. The correlations between different landscape features and visual perception were investigated. On this basis, the data on the landscape gardens of the waterfront greenways of Beijing's second ring water system were visualized in ArcGIS to analyze the spatial distribution characteristics of the riverfront landscape gardens and to propose future development suggestions.

$$y = \beta_0 + \beta_1 x_1 + \cdots + \beta_n x_n + \grave{o} \quad (9)$$

Where y is the visual perception score, $\beta_0, \beta_1, \cdots, \beta_n$ is the regression parameter, x is the impact factor and $\grave{o}$ is the residual.

In this study, the five convolutional neural network models provided by the Wolfram Neural Net Repository were selected for MXNet-based encapsulation to recognize and classify different objects in panoramic images, and the recognition results of each model were compared for vegetation.

IV. Comparison of the results of different models

On March 6, 2019, panoramic images were taken on campus using the Garmin VIRB 360 panoramic camera and analysed for recognition by each of the above-mentioned convolutional neural networks, resulting in a full image resolution of 5,640 × 2,820 pixels. To improve the speed and efficiency of recognition, the images were compressed to a resolution of 1 600 × 800 pixels and converted to an isometric cylindrical projection image for recognition. To quantitatively assess the accuracy of each model's recognition, the vegetation extent of the isoproduct panorama was manually identified and converted to a binary image for analysis using image editing software (Fig. 7).

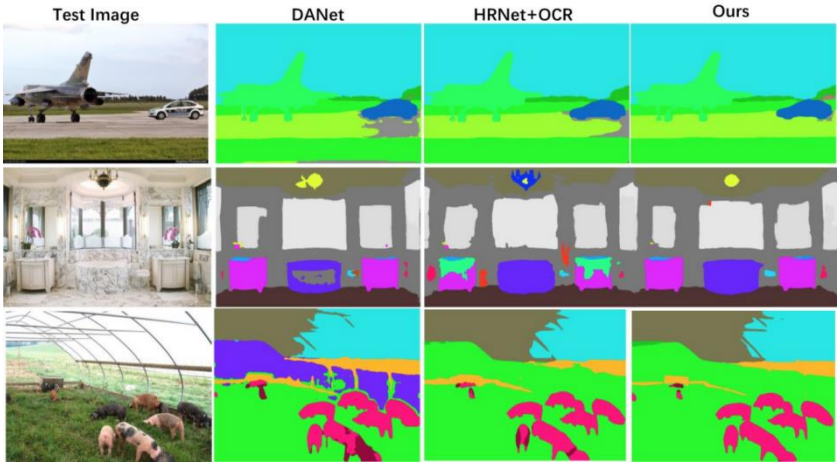

Figure 7 Recognition effect of different CNN models for panoramic images

In general, for the identification of tree parts, the relevant neural network identifies all the area occupied by tree branches as vegetation parts, and does not classify the pores between branches and leaves, which results in a 5%-15% higher green view rate for each model than the manually calibrated data according to the traditional green view area discrimination method for panoramas with a large number of branch pores. However, the fact that the neural network does not recognise the smaller gaps in the vegetation reduces the effect of changes in leaf number, colour and morphology between seasons, thus maintaining consistency in recognition and assessment results between seasons.

The differences between the different models are mainly in the recognition of the near-field lawn and the top cover space; Ademxapp Model A1 is not accurate in the recognition of the far-field vegetation; Dilated ResNet-22 has a large error in the recognition of the vegetation in the cover space and incorrectly identifies some of the surface paving as vegetation, Multi- scale Context Aggregation Net model was not accurate enough to identify vegetation in the landscape and cover space. In order to quantitatively evaluate the accuracy of the calculation results of each

neural network, the IoU of the green areas identified by each neural network was calculated using the manually identified vegetation areas as the standard data (ground truth).

Based on the results of the m IoU calculation (Table 1), the accuracy of each model in descending order was: Dilated ResNet-105>Dilated ResNet-38>Multi-scale Context Aggregation Net>Ademxapp Model A1>Dilated Res Net- 22. Therefore, this study uses Dilated ResNet-105 to conduct an empirical study of green ratings measurement.

Table 1 Comparison of IoU of neural network models for partial identification of green spaces

Name of neural network	IoU-1	IoU-2	IoU-3	IoU-4	mIoU
Adem xapp Model Al	67.00	67.96	71.64	59.33	66.48
Dilated Resnet-22	58.72	62.52	72.88	64.92	64.76
Dilated Resnet-38	69.04	67.48	75.04	66.83	69.60
Dilated Resnet-105	69.49	68.42	75.75	65.98	69.91
Multi-scale context Aggregation Net	70.88	61.48	77.50	64.99	68.71

V. EMPIRICAL EVIDENCE OF PANORAMIC GREEN-VISIBILITY MEASUREMENTS

Based on the aforementioned method of assessing panoramic greenery, Ziyang Park in Wuhan was selected to measure and assess the panoramic greenery of the park at all levels of the park paths and activity plazas. Ziyang Park is a comprehensive park located in Wuhan's Wuchang District, named after Ziyang Lake. The park covers an area of approximately 28.0 h m^2 , of which approximately 11.7 h m^2 is water and 16.3 h m^2 is land.

A. Sample point selection

The panoramic image was taken on Tuesday 12 March 2019 from 09:30-15:30, during which time there were fewer visitors, which reduced the interference of visitors to the measurement during the shooting. The average temperature on the day of the shooting was 16°C, the lighting conditions were good, and the deciduous trees in the park were still in the budding stage, the branches were not yet very dense and the depression was low.

Points were selected at equal distances based on areas accessible to visitors to Ziyang Park. Photographs were taken at 30 m intervals along the centreline of the paths, road intersections and squares at all levels to obtain a panoramic view of the greenery in the different activity areas. Areas within the site that are not accessible to visitors, such as the water and the interior of the planting areas, were not photographed. Due to the closure of the lake island and the central section of Ziyang Lake during the shooting period, access was not possible. A total of 126 filming locations were obtained (Figure 8).

Fig. 8 Scope of the study.

B. Image data recognition and computation

After obtaining the image data, the isometric cylindrical projection of the original image was converted to an isoprojected cylindrical projection, and the green vegetation portion of the panoramic image was identified and calculated using the Dilated ResNet-105 convolutional neural network (Table 2).

Table 2 Results of panoramic green view recognition based on CNN

Type	Green vision rate /%	Total number of samples	Average green vision rate /%
Activity square	56.26	5	36.8
Primary Garden Road	36.25	62	41.93
Secondary Garden Road	32.2	42	54.5
Tertiary Garden Road	85.15	14	66.32
Garden entrance	50.01	3	47.91

Based on the Dilated ResNet-105 convolutional neural network, the panoramic green view of the entrances and exits of Ziyang Park, the paths at all levels and the activity plaza were identified and calculated (Figure 9). The average panoramic green view rate of the park's visitable areas was calculated to be 51.18% based on a combination of sample points across the park. In terms of the spatial distribution of panoramic greenery, there is little variation in greenery across the paths. The highest average panoramic greenery is found on the tertiary roads, the lowest on the activity plaza, the highest on the northern and southern sections of the main park road, and slightly lower on the southeastern and northwestern sections. The average greenery in the area is, in descending order, Tertiary Road > Secondary Road > Park Entrance > Primary Road > Activity Square. In terms of the park as a whole, the highest greenery rate is 85.42% and the lowest 21.19%. The highest greenery rate is on Level 3 Road, which is a paved walk on a large lawn with tall trees and high top vegetation cover.

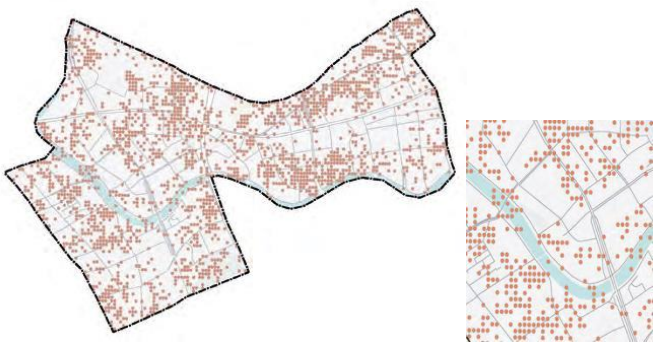

Fig. 9 Analysis of the panoramic green view

The lowest point of green vision is located on a secondary road, surrounded by a large area of water, with vegetation far from the camera lens. Therefore, the proportion of green vegetation is low during the recognition of the images.

C. Comparison of Green Vision Recognition Results

In order to measure the accuracy of the convolutional neural network's green-visibility recognition, the green-visibility of 126 panoramic images was also calculated manually in this study. The vegetation areas of the panoramic images in the isometric cylindrical projection were manually labelled and converted to binary images by image editing software, and the corresponding green-visibility rates were calculated based on the area percentages. The Io U of the vegetation areas identified by the neural network was calculated using the Io U of each image as the horizontal coordinate, and the neural network-identified and manually-identified green-visibility rates as the vertical coordinates to produce a scatter plot (Fig. 10).

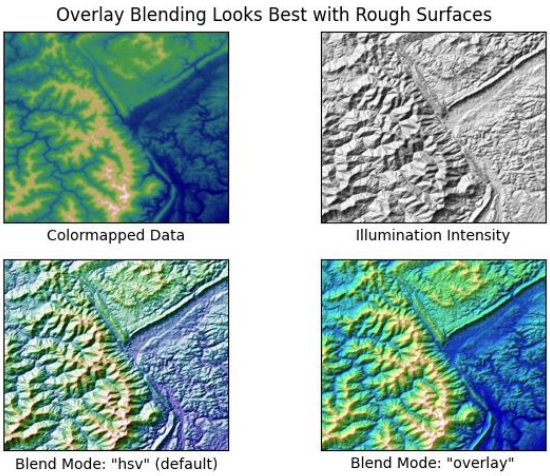

Fig. 10 Distribution of the green view rate of CNN recognition and manual recognition under different IoU

The analysis showed that the IoU of green area recognition using Dilated ResNet-105 convolutional neural network ranged from 33.13% to 83.68%, with an mIoU of 62.53%. The difference between the IoU of the neural network and the IoU of manual recognition ranged from 0.40% to 23.86%, with an average difference of 9.17%. The higher the IoU of the image recognition, the lower the average deviation of the corresponding green-vision rate (Table 3).

Table 3 Comparison of Convolutional Neural Network Recognition and Manual Recognition

Lou range /%	Number of panoramic photos	Percentage of panoramic photos /%	Average deviation of panoramic green viewing rate /%
30-40	3	2.38	14.15
40-50	19	15.08	13.19
50-60	23	18.25	9.92
60-70	46	36.51	8.95
70-80	29	23.02	6.66
80-90	6	4.76	4.82
Total	126	100	9.17

In order to analyse the reasons for the differences between the convolutional neural network recognition results and the manual recognition results, the binary images of the vegetation areas were compared between the two (Table 4).

Table 4 Comparison of recognition results for selected images

Drawing No	IoU/%	Convolution neural network recognition picture (panoramic green viewing rate /%)	Manually recognized pictures (panoramic green viewing rate /%)
1	33.13	41.85	32.7
2	44.79	44.79	43.15
3	55.24	49.51	35.54
4	65.82	49.06	38.34
5	75.41	62.89	61.11
6	83.68	40.81	41.21

Due to the convention of semantic segmentation labelling operations, convolutional neural networks will recognise the porous parts between the branches of trees as vegetation. Traditional manual recognition methods, on the other hand, tend not to include the porous parts of plants because of the significant difference between the colour of the

plant pores and the vegetation. This leads to significant differences in the identification results for sparsely branched trees. For densely foliated vegetation, the results are closer to each other.

In addition, the neural network models selected for this study were trained using Cityscapes landscape garden data, a dataset derived from German urban landscape gardens, which is somewhat different from the Chinese park environment. For the panoramas in cylindrical projection, the accuracy of recognition is affected by the distortion of the relevant elements. During the recognition of some of the panoramas, the model may mistakenly identify the projections of tree branches on the ground, reflections in the water, etc. as vegetation, or may not recognise parts of the lawn due to topographical changes. The tripod at the base of the camera inevitably partially obscures the bottom range of the panorama during the shooting process, which has an impact on some of the results.

VI. Conclusion

The existing open source SegNet image semantic recognition technology has shortcomings for image recognition of riverfront landscape gardens. This paper draws on the method of using landscape garden maps and SegNet to process images for landscape garden feature analysis in the study of street landscape gardens, and combines the image semantic segmentation techniques in deep learning algorithms to train a panoramic image segmentation model applicable to riverfront greenways, with an accuracy of 0.93 and an MIoU of 0.74, which is accurate for batch processing of urban riverfront greenway images and has universal applicability. The image segmentation results can provide designers, planners, public environment researchers and other experts in the field with effective methods for quantifying riverine landscapes, and provide strong support for human-scale riverine landscape planning, design and multi-stakeholder research.

Acknowledgment

This work no funding supported.

References

[1] Xiao, Y., Miao, S., Zhang, Y., Chen, H., & Wenjie, W. U. (2021). Exploring the health effects of neighborhood greenness on Lilong residents in Shanghai. Urban Forestry & Urban Greening, 66, 127383.

[2] Virtanen, J. P., Jaalama, K., Puustinen, T., Julin, A., Hyyppä, J., & Hyyppä, H. (2021). Near Real-Time Semantic View Analysis of 3D City Models in Web Browser. ISPRS International Journal of Geo-Information, 10(3), 138.

[3] Ergen, M. (2021). Using geographical information systems to measure accessibility of green areas in the urban center of Nevşehir, Turkey. Urban Forestry & Urban Greening, 62, 127160.

[4] Su, J., Zhang, R., Zhao, X., Chinkam, O. N., Zhang, H., Li, F., & Kang, L. (2021). A Multi-source Data Based Analysis Framework for Urban Greenway Safety. Tehnički vjesnik, 28(1), 193-202.

[5] Ergen, M. (2021). Using geographical information systems to measure accessibility of green areas in the urban center of Nevşehir, Turkey. Urban Forestry & Urban Greening, 62, 127160.

[6] Yang, Y., Lu, Y., Yang, H., Yang, L., & Gou, Z. (2021). Impact of the quality and quantity of eye-level greenery on park usage. Urban Forestry & Urban Greening, 60, 127061.

[7] Soba, D., Gámez, A. L., Úriz, N., de Larrinaga, L. R., Gonzalez-Murua, C., Becerril, J. M., ... & Aranjuelo, I. (2021). Foliar heavy metals and stable isotope (δ 13C, δ 15N) profiles as reliable urban pollution biomonitoring tools. Urban Forestry & Urban Greening, 57, 126918.

[8] Hu, T., Wei, D., Su, Y., Wang, X., Zhang, J., Sun, X., ... & Guo, Q. (2022). Quantifying the shape of urban street trees and evaluating its influence on their aesthetic functions based mobile lidar data. ISPRS Journal of Photogrammetry and Remote Sensing, 184, 203-214.

[9] Falfán, I., Muñoz-Robles, C. A., Bonilla-Moheno, M., & MacGregor-Fors, I. (2018). Can you really see ‘green’? Assessing physical and self-reported measurements of urban greenery. Urban Forestry & Urban Greening, 36, 13-21.

[10] Jessup, K., Parker, S. S., Randall, J. M., Cohen, B. S., Roderick-Jones, R., Ganguly, S., & Sourial, J. (2021). Planting Stormwater Solutions: A methodology for siting nature-based solutions for pollution capture, habitat enhancement, and multiple health benefits. Urban Forestry & Urban Greening, 64, 127300.

[11] Guan, C., Song, J., Keith, M., Zhang, B., Akiyama, Y., Da, L., ... & Sato, T. (2021). Seasonal variations of park visitor volume and park service area in Tokyo: A mixed-method approach combining big data and field observations. Urban Forestry & Urban Greening, 58, 126973.

[12] Zhang, J., Zhao, X., Chen, Z., & Lu, Z. (2019). A review of deep learning-based semantic segmentation for point cloud. IEEE Access, 7, 179118-179133.

[13] Langsetmo, L., Kats, A. M., Cawthon, P. M., Cauley, J. A., Vo, T. N., Taylor, B. C., ... & Osteoporotic Fractures in Men (MrOS) Study Group. (2019). The association between objectively measured physical activity and subsequent health care utilization in older men. The Journals of Gerontology: Series A, 74(6), 820-826.

[14] Ye, Y., & Qiu, H. (2021). Environmental and social benefits, and their coupling coordination in urban wetland parks. Urban Forestry & Urban Greening, 60, 127043.

[15] Wu, W., Yun, Y., Hu, B., Sun, Y., & Xiao, Y. (2020). Greenness, perceived pollution hazards and subjective wellbeing: Evidence from China. Urban Forestry & Urban Greening, 56, 126796.

[16] Zhou, Q., Yang, W., Gao, G., Ou, W., Lu, H., Chen, J., & Latecki, L. J. (2019). Multi-scale deep context convolutional neural networks for semantic segmentation. World Wide Web, 22(2), 555-570.

[17] Wu D, Zhang C, Ji L, et al. Forest Fire Recognition Based on Feature Extraction from Multi-View Images[J]. Traitement du Signal, 2021, 38(3): 775-783.

[18] Li, H., Xie, H., & Woodward, G. (2021). Soundscape components, perceptions, and EEG reactions in typical mountainous urban parks. Urban Forestry & Urban Greening, 64, 127269.

[19] Soininen, L., Grönroos, M., Roslund, M. I., & Sinkkonen, A. (2021). Long-term storage affects resource availability and occurrence of bacterial taxa linked to pollutant degradation and human health in landscaping materials. Urban Forestry & Urban Greening, 60, 127065.

[20] Hao, S., Zhou, Y., & Guo, Y. (2020). A brief survey on semantic segmentation with deep learning. Neurocomputing, 406, 302-321.

[21] Zhengwan, Z. H. A. N. G., Chunjiong, Z. H. A. N. G., Hongbing, L. I., & Tao, X. I. E. (2020). Multipath transmission selection algorithm based on immune connectivity model. Journal of Computer Applications, 40(12), 3571. DOI: 10.11772/j.issn.1001-9081.2020040492

[22] Liu, Z., Li, X., Luo, P., Loy, C. C., & Tang, X. (2017). Deep learning markov random field for semantic segmentation. IEEE transactions on pattern analysis and machine intelligence, 40(8), 1814-1828.

[23] Chen, K., Fu, K., Yan, M., Gao, X., Sun, X., & Wei, X. (2018). Semantic segmentation of aerial images with shuffling convolutional neural networks. IEEE Geoscience and Remote Sensing Letters, 15(2), 173-177.